



Electron-tunneling measurements of low- T_c single-layer $\text{Bi}_{2+x}\text{Sr}_{2-y}\text{CuO}_{6+\delta}$: Evidence for a scaling disparity between superconducting and pseudogap states

Th. Jacobs,¹ S. O. Katterwe,¹ H. Motzkau,¹ A. Rydh,¹ A. Maljuk,² T. Helm,³ C. Putzke,⁴ E. Kampert,⁵ M. V. Kartsovnik,³ and V. M. Krasnov^{1,*}

¹*Department of Physics, Stockholm University, AlbaNova University Center, SE-10691 Stockholm, Sweden*

²*Leibniz Institute for Solid State and Materials Research IFW Dresden, Helmholtzstrasse 20, D-01171 Dresden, Germany*

³*Walther-Meißner-Institut, Bayerische Akademie der Wissenschaften, Walther-Meißner-Strasse 8, D-85748, Garching, Germany*

⁴*H. H. Wills Physics Laboratory, University of Bristol, Tyndall Avenue, Bristol, BS8 1TL, United Kingdom*

⁵*Helmholtz-Zentrum Dresden-Rossendorf, Hochfeld-Magnetlabor Dresden, DE-01314 Dresden, Germany*

(Received 22 February 2012; revised manuscript received 29 November 2012; published 12 December 2012)

We experimentally study intrinsic tunneling and high magnetic field (up to 65 T) transport characteristics of the single-layer cuprate $\text{Bi}_{2+x}\text{Sr}_{2-y}\text{CuO}_{6+\delta}$, with a very low superconducting critical temperature $T_c \lesssim 4$ K. It is observed that the superconducting gap, the collective bosonic mode energy, the upper critical field, and the fluctuation temperature range are scaling down with T_c , while the corresponding pseudogap characteristics remain the same as in high- T_c cuprates with 20 to 30 times higher T_c . The observed disparity of the superconducting and pseudogap scales clearly reveals their different origins.

DOI: 10.1103/PhysRevB.86.214506

PACS number(s): 74.55.+v, 74.62.-c, 74.72.Gh, 74.72.Kf

I. INTRODUCTION

An interplay between the normal state pseudogap (PG) and unconventional superconductivity remains a highly debated issue. For high transition temperature cuprates the energy scales of the superconducting gap Δ_{SG} and PG Δ_{PG} are similar (30–50 meV). They are close to several oxygen phonon modes and comparable to the antiferromagnetic exchange energy. It remains unsettled whether this is a mere coincidence, a prerequisite for a high T_c , or an indication of the common origin of Δ_{SG} and Δ_{PG} . Within the precursor superconductivity scenario, the PG is identified with the pairing gap and the apparent difference between the PG onset temperature T^* and the superconducting transition temperature T_c is attributed to large phase fluctuations.^{1,2} In an alternative two-gap scenario the pseudogap represents a different order coexisting and competing with superconductivity.^{3–10} The extent of superconducting fluctuations is determined by the ratio of Δ_{SG} to the Fermi energy E_F and the dimensionality of the system.¹¹ Cuprate superconductors have homologous series of compounds with a different number of CuO planes per unit cell. Within each series the Fermi energies,^{12–15} resistivities, anisotropies, and dimensionality are similar,^{16–18} but exhibit a large variation of T_c , whose origin remains a major challenge. Since thermal fluctuations vanish at $T \rightarrow 0$, they should be less significant at $T \sim T_c$ in low- T_c cuprates. Therefore it is instructive to study superconducting and pseudogap characteristics in cuprates with very low T_c .

In this work we present combined intrinsic tunneling and transport measurements of $\text{Bi}_{2+x}\text{Sr}_{2-y}\text{CuO}_{6+\delta}$ (Bi-2201) single crystals with low $T_c \lesssim 4$ K. Bicuprates represent stacks of atomic-scale intrinsic Josephson junctions^{19–22} which facilitates measurements of bulk electronic spectra by means of intrinsic tunneling spectroscopy.^{4,20,23,24} We observe that all superconducting characteristics are reduced in proportion to T_c , but the corresponding c -axis pseudogap characteristics remain similar to that in high- T_c Bi-2212²³ and Bi-2223²⁰ compounds with 20–30 times larger T_c . The disparity of the superconducting and pseudogap scales in Bi-2201 clearly reveals their different origins.

The paper is organized as follows. In Sec. II we describe the sample fabrication and the experimental method. In Sec. III we present the main experimental results for the studied Bi-2201 crystals, including intrinsic tunneling spectroscopy, magnetotunneling, and transport measurements at different temperatures and magnetic fields. In Sec. IV we show representative intrinsic tunneling data for double-layer Bi-2212 crystals. Finally, in Sec. V we argue that the observed large disparity between superconducting and pseudogap scales is inconsistent with the precursor model of the pseudogap and discuss the extent of fluctuations and mechanisms of large variation of T_c within homologous families of cuprates.

II. EXPERIMENT

$\text{Bi}_{2+x}\text{Sr}_{2-y}\text{CuO}_{6+\delta}$ crystals with $x = 0.15$ and $y = 0.1$ were grown by the traveling solvent floating zone technique.²⁵ The T_c of $\text{Bi}_{2+x}\text{Sr}_{2-y}\text{CuO}_{6+\delta}$ depends not only on oxygen doping δ , but also on the Bi and Sr content; the stoichiometric $x = y = 0$ compound is nonsuperconducting. Our as-grown crystals were overdoped (OD) with $T_c \simeq 3.5$ K. Most measurements were done in a flowing gas ⁴He cryostat at $1.8 < T < 300$ K and a magnetic field up to 17 T, or a ³He cryostat with T down to 270 mK and a field up to 5 T. Complementary measurements were made in pulsed magnetic fields up to 65 T. In all cases, magnetic field was applied along the c -axis direction.

Small mesa structures, containing few intrinsic junctions, were fabricated on top of freshly cleaved crystals, allowing measurements of both ab plane and c -axis characteristics. To obviate self-heating,²⁶ we limited the height of the mesas to only a few atomic layers, using slow 250 eV Ar-ion milling, and reduced the mesa areas to submicron sizes with two different miniaturization techniques. In both cases the crystals were glued to a sapphire substrate, cleaved, and immediately covered by a protective gold layer, which also ensured good electrical contact to the crystal.

In the first technique, an elongated line with about a nanometer height was etched at the top of the crystal, using

photolithography and Ar milling. A CaF layer was deposited afterwards and the top of the line was opened using a lift-off process. This enabled an electrical contact to the line, while the rest of the surface was insulated. An additional insulation and planarization layer was made from photoresist to further improve the insulation and even out the height difference between crystal and substrate. Six 200-nm-thick gold contact fingers, perpendicular to the line, were then fabricated by *e*-beam evaporation, photolithography, and Ar milling. The Ar milling also etched the crystal surface between the fingers, resulting in moderately large mesas underneath the fingers at the crossing with the line, with an area of approximately $6 \times 8 \mu\text{m}^2$. To further reduce the area, each mesa could be trimmed into two smaller ones using a focused ion beam. One large and two trimmed mesas made by this technique are shown in Fig. 1(a).

In the second technique, six different sized Pt/C etching masks were patterned on the crystal, using (focused) electron beam induced deposition in a dual-beam SEM/FIB system. Then only a few atomic layers of crystal surface were removed by Ar milling, resulting in mesas with areas of ~ 0.6 to $2.5 \mu\text{m}^2$. To improve the conductance of the masks, the carbon content was reduced using O-plasma ashing. An insulation and planarization layer, made from photoresist, was fabricated afterwards. The natural passivation layer that forms on uncovered parts of the crystal surface after cleaving acted as an additional insulation. Six Au contact fingers were then made using *e*-beam evaporation, photolithography, and Ar milling.

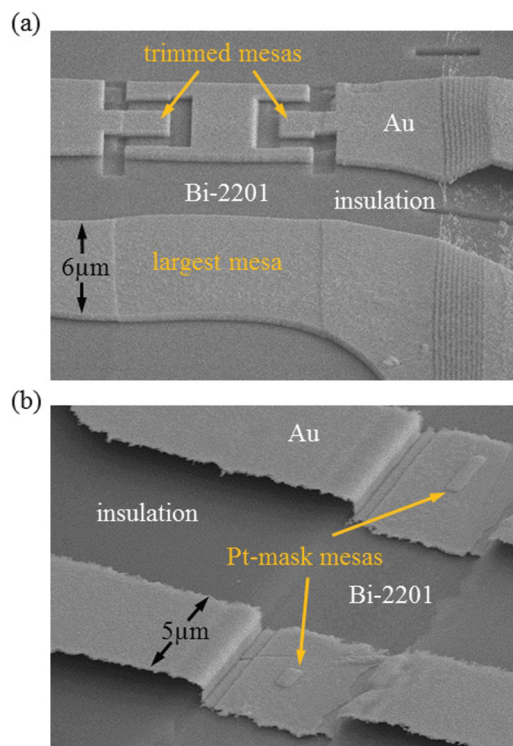


FIG. 1. (Color online) SEM images of Bi-2201 mesa structures made by two different techniques. The mesa areas were reduced to submicron sizes using (a) FIB trimming of moderately large mesas or (b) by fabricating small Pt masks using (focused) electron beam induced deposition.

They completely cover the mesas, which further improves their thermal properties. Two mesas made by this technique are shown in Fig. 1(b).

In both cases, the contact fingers lead to 12 larger bonding pads on the substrate. The samples were mounted on a sample holder and contacted with bonding wires. The contact configuration allows either three- or four-terminal measurements of *c*-axis characteristics of mesas and four-terminal in-plane measurements of the underlying base crystal.

III. RESULTS

A. Intrinsic tunneling

Figure 2(a) shows the zero-bias *c*-axis resistance $R_c(T)$ for different mesas. Mesas made by the first technique show a metallic behavior at high T , which turns into semiconductinglike with a minimum at $T^* \sim 90$ K, while mesas made by the second technique exhibit a higher $T^* \simeq 170$ K. By comparing with reported doping dependencies of $R_c(T)$ for Bi-2201,^{17,27} we conclude that the former crystal is optimally doped (OP), while the latter became slightly underdoped (UD) due to partial out-diffusion of oxygen during fabrication. This is accompanied by a systematic variation of the critical temperature from $T_c \simeq 3.5$ K for as-grown overdoped crystals to $T_c = 4.3 \pm 0.3$ K (OP) and 3.8 ± 0.4 K (UD) for crystals made by the first and second technique, respectively. From Fig. 2(a) it is clear that the T^* grows rapidly with underdoping, consistent with the existence of a critical doping point.^{3,4,7,9,21,27}

Figure 2(b) shows current density-voltage (*J*-*V*) characteristics of two OP mesas with different sizes, on the same crystal. It is seen that the large OP mesa does show a clear critical current. Since our measurements are quasi-four probe, the smallest measured resistance $R_c(V = 0 \text{ V})$ is nonzero and is determined by the contact resistance between the Au electrode and the top of the mesa. It is usually of the order of the resistance of one intrinsic junction [see, e.g., Fig. 1(a) in Ref. 23]. From Fig. 2(b) it is seen that for the smaller mesa the high-bias resistivity remains the same. The critical current density is also the same but is significantly smeared out. Since both the critical current density and the large bias resistivity are independent of the mesa area, the apparent larger zero-bias resistivity at $T < T_c$ for small mesas, visible in Fig. 2(a), is not caused by deterioration of the contact but is due to enhanced thermal fluctuations, leading to phase diffusion²⁸ in the smallest mesas. The true (unaffected by fluctuations) level of the contact resistance corresponds to that for the larger mesa in Fig. 2(a) at $T < T_c$.

Figure 2(c) shows the *I*-*V* characteristics of a small UD mesa at different T and H . Here the supercurrent is almost completely suppressed by thermal fluctuations due to the much smaller size of the junctions and because the critical current density is rapidly decreasing with underdoping.⁴ At a larger bias ~ 5 mV we observe a kink in the *I*-*V*, which appears only in the superconducting state and is easily suppressed both by temperature at $T > T_c$ and by a modest *c*-axis magnetic field.

Figure 2(d) shows intrinsic tunneling conductances $dI/dV(V)$ (in the semilogarithmic scale) for six mesas with areas from $A = 0.6 \pm 0.2$ to $2.5 \pm 0.3 \mu\text{m}^2$ on the same crystal. The peak-dip features in the $dI/dV(V)$ s correspond

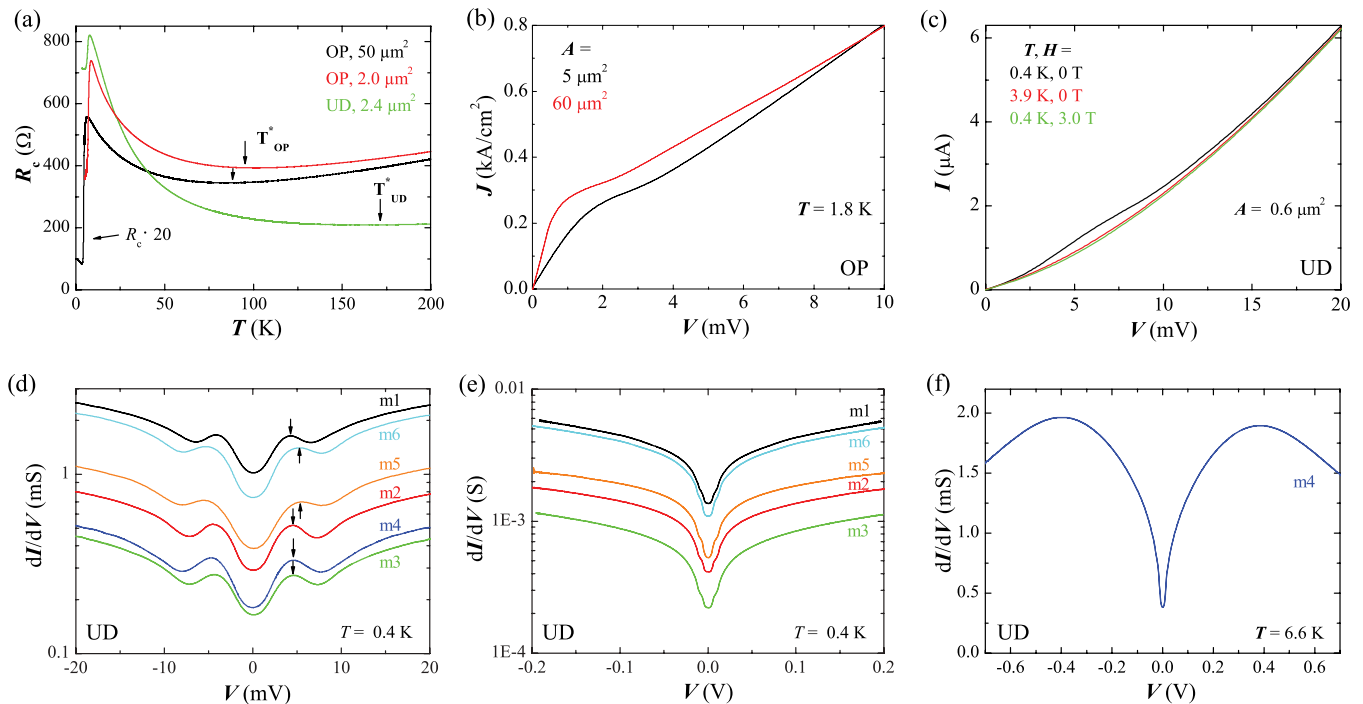


FIG. 2. (Color online) (a) Zero bias c -axis resistances for a large and small OP mesa and a small UD mesa. The pseudogap onset temperatures T^* are indicated by downward arrows. (b) J - V characteristics for two OD mesas with different sizes. J_c smears out for reduced mesa areas due to fluctuations, leading to nonzero $R_c(T < T_c)$ for very small mesas. (c) I - V s for a small UD mesa, showing a sum-gap kink which appears only in the superconducting state and corresponds to peak-dip features in the $dI/dV(V)$ characteristics. (d) Intrinsic tunneling conductances (in the semilog scale) at 400 mK for UD mesas with different areas from $0.6 \pm 0.2 \mu\text{m}^2$ (m3) to $2.5 \pm 0.3 \mu\text{m}^2$ (m1), fabricated on the same crystal. Downward and upward arrows mark sum-gap peaks for mesas with $N = 5$ and 6 junctions, respectively. (e) Large bias $dI/dV(V)$ curves for the same mesas as in (d). It is seen that the curves also retain the same size-independent shape at larger bias, despite a significant difference in mesa sizes and power dissipation, implying that they are not significantly distorted by self-heating. (f) $dI/dV(V)$ at 6.6 K for one of the smallest mesas at even larger bias. The hump voltage corresponds to the c -axis pseudogap $\Delta_{\text{PG}} \sim 40$ meV.

to the kink in the I - V s, with a power at the peaks varying from ~ 1.2 to $7.4 \mu\text{W}$. Figure 2(e) presents similar data for larger bias. It is seen that the $dI/dV(V)$ characteristics retain the same shape (in the semilogarithmic scale) for all mesas, independent of mesa area and dissipation power. This shows that the mesa conductance is scaling by a simple factor, proportional to the mesa area. The size independence of the shape is a clear indication that there is no significant distortion by self-heating, even at larger bias, since self-heating should be larger for larger mesas with higher dissipation power, which would lead to a size dependence of self-heating artifacts.^{23,26}

The peak-dip structure seen in the $dI/dV(V)$ s is typical for tunneling characteristics of (underdoped) cuprates.^{4,29-33} The peak is attributed to the superconducting sum-gap singularity at $V_{\text{peak}} = 2\Delta_{\text{SG}}N/e$, where N is the number of junctions in the mesa.^{23,24} The dip is usually ascribed to a collective bosonic mode with energy $\Omega_B = eV_{\text{dip}} - 2\Delta_{\text{SG}}$ (per junction).^{29,30} The corresponding ratio $\Omega_B/2\Delta_{\text{SG}} = V_{\text{dip}}/V_{\text{peak}} - 1 \simeq 0.62$ in our crystals is close to the average value $\simeq 0.64$, deduced from inelastic neutron scattering for different cuprates.³⁴ However, to obtain Δ_{SG} and Ω_B we need to estimate N . For high- T_c Bi-2212²³ this is simply done by counting quasiparticle branches in the I - V [see the inset in Fig. 5(a)]. However, in low- T_c Bi-2201 the branches are not distinguishable.²¹

Still it is possible to estimate N by comparing mesas with different heights. The uniformity of Ar milling is in the same range as the interlayer spacing s , the mesas on the same crystal may therefore have either N or $N + 1$ junctions. In Fig. 2(d) this is seen as two sets of peaks, marked by downward and upward arrows. Assuming that the ratio of voltages is $(N + 1)/N$, we obtain $N = 5$. This corresponds to the large bias [$V \simeq 20$ mV in Fig. 2(d)] c -axis resistivity $\rho_c = RA/Ns \simeq 20 \Omega \text{ cm}$, consistent with the expected value.^{4,21,27} Thus we obtain $\Delta_{\text{SG}} = eV_{\text{peak}}/2N = 0.55 \pm 0.1$ meV and $2\Delta_{\text{SG}}/k_B T_c = 3.5 \pm 0.6$, typical for weak-coupling superconductors and consistent with previous studies on Bi(La)-2201 with a higher T_c .^{21,29,32,35} The bosonic mode energy $\Omega_B \simeq 0.7$ meV is also small and clearly not related to the much higher phonon or antiferromagnetic exchange energies. Rather, Ω_B is determined solely by $\Delta_{\text{SG}}(T)$, consistent with an interpretation of the mode as an exciton of Bogoliubov quasiparticles in a d -wave superconductor.³⁶

Figure 2(f) shows a $dI/dV(V)$ of the UD mesa m4 at even larger bias and at $T = 6.6 \text{ K} > T_c$. It is seen that the $dI/dV(V)$ is V-shaped above T_c , generic for the PG state.^{23,37} A PG hump appears at $V_{\text{hump}} \simeq 0.4$ V, for $N = 5$ this corresponds to $\Delta_{\text{PG}} \simeq 40$ meV. Obviously, for our Bi-2201 not only $T^* \simeq 170 \text{ K} \gg T_c \simeq 4 \text{ K}$, but also $\Delta_{\text{PG}} \simeq 40 \text{ meV} \gg \Delta_{\text{SG}} \simeq 0.55 \text{ meV}$.

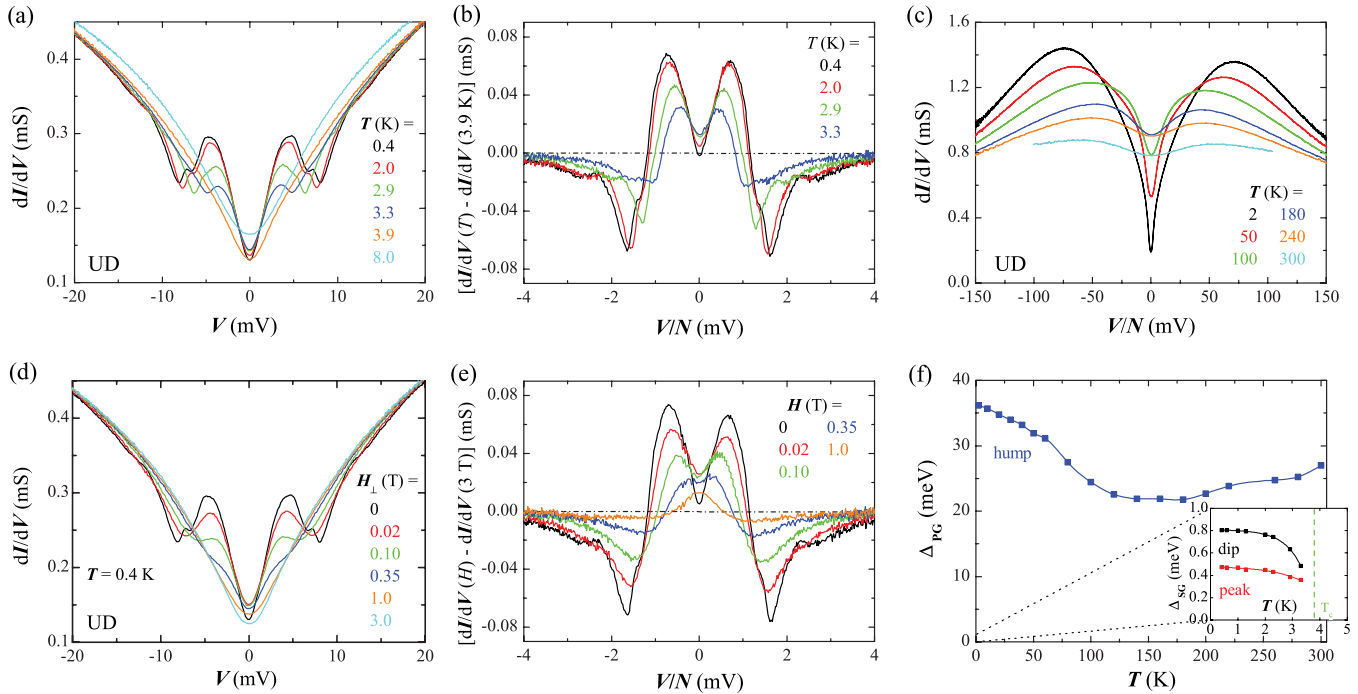


FIG. 3. (Color online) (a) Temperature dependence of intrinsic tunneling characteristics for the smallest UD mesa m3 at $H = 0$ T. It is seen that both the peak and dip disappear at $T \rightarrow T_c$. (b) Data from (a) with a subtracted V-shaped PG background at $T \simeq T_c$ and with voltage normalized per intrinsic junction. (c) T dependence of the PG characteristics at $T > T_c$ for another UD mesa with the same area as in (a). (d) Magnetic field dependence of $dI/dV(V)$ curves for the UD mesa m3 at $T = 400$ mK. The peak-dip structure disappears in a field of a few Tesla. (e) Data from (d) with a subtracted pseudogap background at $H = 3$ T. (b) and (e) demonstrate that the peak and the dip are suppressed in a similar correlated manner both by temperature and by magnetic field. They also show that the dip is indeed a dip with a negative conductance compared to the normal state PG background. (f) Temperature dependence of the pseudogap, obtained from half of the hump voltage in (c). The inset shows the T dependence of the superconducting gap, obtained from 1/2 of the peak and dip voltages, from (a). The superconducting gap decreases in a mean-field BCS manner both with increasing T and H , but the pseudogap is much less insensitive to T and H .

B. Temperature and magnetic field dependence

Figure 3(a) shows the T dependence of the $dI/dV(V)$ for the smallest UD mesa m3 at $H = 0$ T. To improve the resolution, we present the same data with a subtracted normal state background⁴ in Fig. 3(b). It is seen that both the peak and the dip are suppressed in the BCS manner (flat at $T \ll T_c$ and a fast decay at $T \rightarrow T_c$) with increasing T and magnetic field, see Fig. 3(d). The inset in Fig. 3(f) shows the temperature dependence of the superconducting gap obtained from half of the peak voltage. It decreases with increasing T and vanishes at T_c . Here we also show half of the dip voltage. It is seen that the difference between the peak and dip voltages, which should represent the frequency of the collective bosonic mode, is also vanishing at $T \rightarrow T_c$, similar to $\Delta_{SG}(T)$. Apparently the frequency of the bosonic mode is intimately related to the superconducting gap, which is not expected for antiferromagnetic magnons. This observation supports the interpretation of the mode as an exciton of Bogoliubov quasiparticles in a d -wave superconductor, not necessarily related to possible magnetism in the material.³⁶

From the $dI/dV(V)$ characteristics it is clear that the V-shaped PG coexists with superconductivity at $T < T_c$.^{23,37} This makes it difficult to separate superconducting and PG-related phenomena below T_c by looking solely on the T variation of experimental characteristics. However, such a

separation can be done by studying magnetic field effects.²⁴ The upper critical field for the suppression of spin-singlet superconductivity H_{c2} is limited by the paramagnetic (Zeeman) effect, $H_{c2}(0)/T_c \sim 2.2$ T/K for weak coupling d -wave superconductors.³⁸ Therefore, H_{c2} for low- T_c Bi-2201 should be much lower and easier accessible than for high- T_c Bi-2212 with $H_{c2} \sim 100$ T.^{10,24}

Figure 3(d) shows the effect of a H variation to the $dI/dV(V)$ for the same mesa as in Fig. 3(a). Figure 3(e) shows the same data with a subtracted background at large field. It is clear that the peak and the dip are suppressed in a correlated manner with increasing H . The tunneling MR remains significant at a dissipation power about an order of magnitude larger than at the peak, implying that the sample remains at $T < T_c$ and confirming the lack of significant self-heating at the peak.

Figure 3(c) shows the T dependence of the PG characteristics at $T > T_c$ for another UD mesa with a similar size. The PG hump is smeared out at $T \rightarrow T^* = 170$ K, but is still visible even at higher T . The main panel in Fig. 3(f) shows the temperature dependence of the pseudogap, obtained from half the hump voltage. Both the value of the PG and its T dependence are remarkably similar to that for Bi-2212 (see Fig. 5 and Refs. 4,21,23, and 37), despite a more than 20 times smaller T_c and Δ_{SG} .

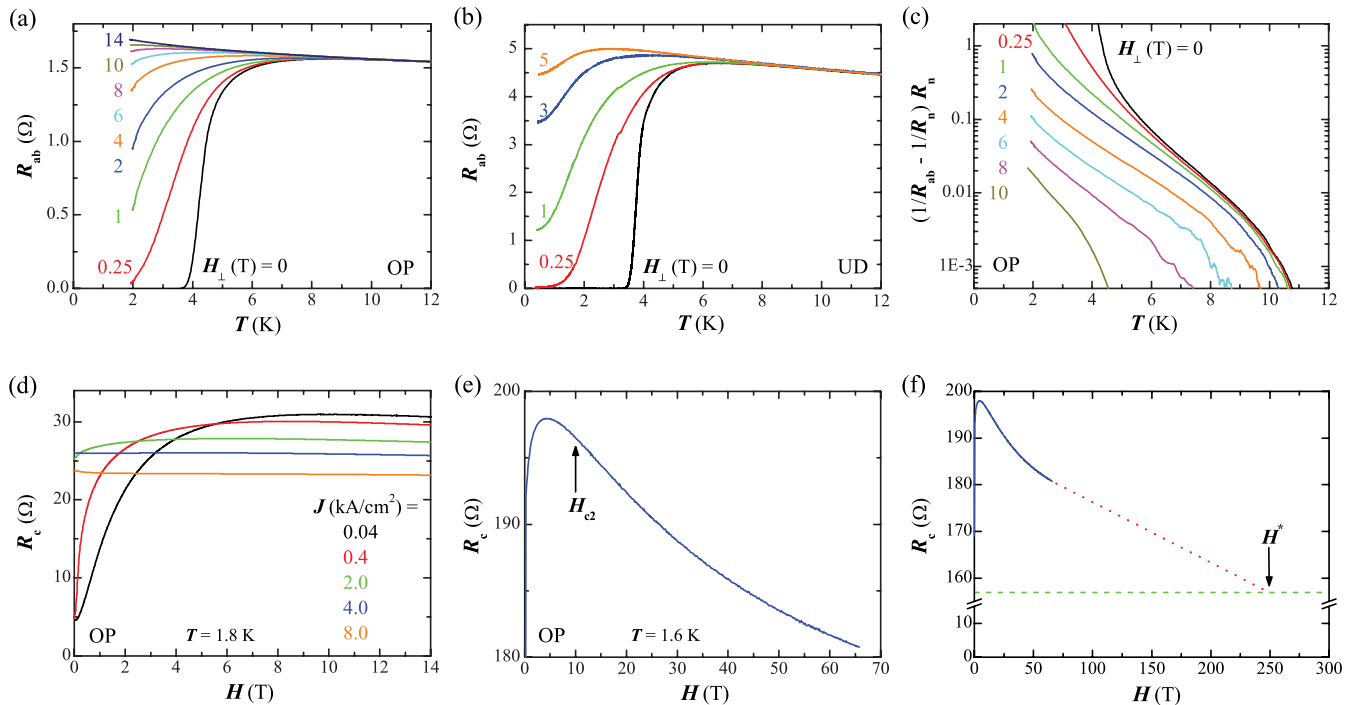


FIG. 4. (Color online) ab -plane resistance at different H for an (a) OP and (b) UD crystal. A complete suppression of T_c at $H_{c2} \simeq 10$ T is seen. (c) Excess fluctuation conductance for the data from (a). It is seen that fluctuations decay rapidly (almost exponentially) with increasing T and that the region of significant fluctuations expand to about twice the T_c . (d) Bias current dependence of the c -axis MR for an OP mesa. The MR is large at small current densities but vanishes at large bias, corresponding to the nearly ohmic tunnel resistance part of the I - V . (e) c -axis MR in a pulsed field, showing a profound negative MR at large fields, which is attributed to the suppression of the pseudogap. (f) Demonstrates an estimation of the PG suppression field $H^* \sim 250 \pm 50$ T by extrapolating the data from (e) to the large bias T - and H -independent tunneling resistance (dashed horizontal line).

C. Transport measurements

Figures 4(a) and 4(b) show in-plane resistances $R_{ab}(T)$ at different H for OP and UD crystals, respectively. The T_c decreases with increasing H . No signature of a superconducting transition is visible at $H > 10$ T. However, a positive in-plane magnetoresistance (MR) persists well above $T_c(H)$, indicating a broad fluctuation region. From magnetotunneling and the combined transport measurements shown in Fig. 3(d), we estimate $H_{c2}(T = 0 \text{ K}) = 10 \pm 2$ T and $H_{c2}(T = 0 \text{ K})/T_c = 2.5 \pm 1$ T/K, consistent with previous reports.^{8,10,16,24} H_{c2} is close to the paramagnetic limit, ruling out a significant underestimation.

Figure 4(c) represents the fluctuation conductance [assuming for the normal state $R_n = R_{ab}(H = 14 \text{ T})$]. The MR falls to less than 1% at $T/T_c(H) \simeq 2.3$, similar to Bi(La)-2201 with higher T_c .²⁷ However, because of the very low T_c it expands only to about $T \sim 10 \text{ K} \ll T^* \simeq 170 \text{ K}$. This shows that the temperature range of superconducting fluctuations is determined by T_c and not by the much larger T^* .

Figure 4(d) shows the bias dependence of the c -axis MR for a larger OP mesa and demonstrates that the MR vanishes at large bias. This is the consequence of state conservation: Well above the sum-gap voltage, the tunnel current should be the same in the superconducting and normal state, leading to a T and H independence of the large bias resistance,²⁴ as seen in Figs. 2(c), 3(a), and 3(d).

Figure 4(e) shows the zero-bias $R_c(H)$ for a small OP mesa, measured in a pulsed field. Two contributions to the

MR are seen: At low fields there is a positive MR due to a suppression of the interlayer supercurrent, as seen in Fig. 4(d). At higher fields a profound negative MR occurs, which does not saturate at 65 T. A very large characteristic field, $H^* \sim 250 \pm 50$ T, is estimated by linear extrapolation to the H - and T -independent tunnel resistance, shown in Fig. 4(f). Even though such behavior has been reported before,^{16,17,39} its interpretation for high- T_c cuprates is obscured by a large $H_{c2} \sim 100$ T.²⁴ In our low- T_c Bi-2201, the superconducting and the pseudogap suppression fields are well separated, $H^* \sim 250 \text{ T} \gg H_{c2} \sim 10 \text{ T}$. The two fields correspond to the Zeeman energy in the order of Δ_{PG} and Δ_{SG} , respectively. This not only supports an estimation of the gaps, but also suggests that both are caused by spin-singlet pairing.³⁹

IV. COMPARISON WITH Bi-2212

In Fig. 5 we show representative data for Y-doped Bi-2212 crystals with optimal $T_c \simeq 95$ K (data from Ref. 23). In Bi-2212, multiple quasiparticle branches are very well visible, as shown in the inset in Fig. 5(a). They are due to one-by-one switching of intrinsic Josephson junctions from the superconducting to the resistive (quasiparticle) state. First of all we note that the PG characteristics Bi-2201 and Bi-2212 are remarkably similar, compare PG characteristics in Figs. 3(c) and 5(b) and in Figs. 3(f) and 5(c).

In the superconducting state there are both similarities and differences. In both Bi-2201 and Bi-2212 the sum-gap peak

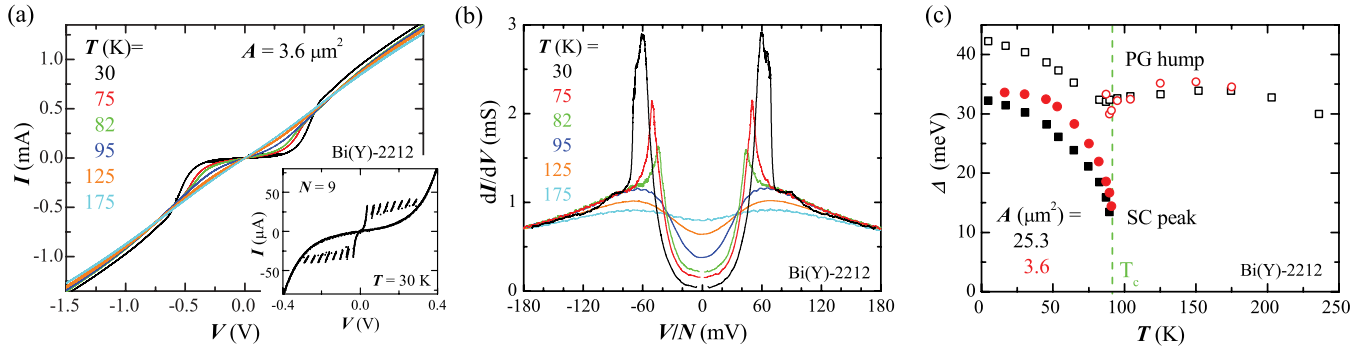


FIG. 5. (Color online) Representative data for Y-doped, Bi-2212 mesas with nearly optimal doping (data from Ref. 23). (a) I - V characteristics at different temperatures and $H = 0$ T for a small Bi-2212 mesa. A pronounced sum-gap kink is seen. The inset shows the low bias part of the I - V at low T . Multiple quasiparticle branches are due to one-by-one switching of intrinsic Josephson junctions from the superconducting to the resistive (quasiparticle) state. (b) $dI/dV(V)$ curves for the data in (a). (c) Temperature dependence of the sum-gap peak and the pseudogap hump voltages per intrinsic junction for mesas with different sizes for the same Bi-2212 crystal. It is seen that the superconducting peak is vanishing in a mean-field BCS manner at $T \simeq T_c$, but the pseudogap survives up to almost room temperature, as also seen from (b). Note that unlike the low- T_c Bi-2201 crystals, the pseudogap and the superconducting gap in high- T_c Bi-2212 have similar energies $\Delta_{SG}(T = 0 \text{ K}) \sim \text{PG} \sim 35\text{--}40$ meV.

vanishes in the mean-field BCS manner above T_c [compare inset in Figs. 3(f) and 5(c)]. However, in Bi-2212 the peak corresponds to a much larger superconducting gap $\Delta_{SG}(T = 0 \text{ K}) \sim 35$ meV, which is close to the PG ~ 40 meV. This fact is often used as an argument in favor of the common origin of the two gaps. However, a comparison with low- T_c Bi-2201 indicates that this is probably a mere coincidence rather than an indication of a precursor superconductivity origin of the pseudogap.

It is also seen from comparison of Figs. 3(a) and 5(b) that in Bi-2212 the superconducting conductance peak is much more pronounced, while the subgap conductance is more suppressed than in Bi-2201. In other words, Bi-2201 intrinsic tunnel junctions are more leaky than Bi-2212 junctions. This implies that the c -axis transport in Bi-2201 is not purely due to single quasiparticle tunneling but also involves a Cooper pair (leakage) transport channel.³⁷ There are several factors for this less two-dimensional behavior of Bi-2201 compared to Bi-2212: (i) The interlayer spacing in Bi-2201 ($s \simeq 1.2$ nm) is smaller than in Bi-2212 ($s \simeq 1.5$ nm) and (ii) the coherence length in Bi-2201 is larger than in Bi-2212, due to a much smaller energy gap. The less-2D behavior of Bi-2201 is indeed obvious from the lack of individual branches in I - V characteristics. Another factor is the presence of a strong pseudogap at low T in Bi-2201, due to which the “normal” state already has a strongly suppressed zero-bias conductance.

The leakiness, that is, the presence of both quasiparticle and Cooper pair contributions,³⁷ also affects the c -axis magnetoresistance in Bi-2201. An application of a magnetic field leads to a negative magnetoresistance for subgap quasiparticles (increase of QP conductance), but to a positive magnetoresistance for pair transport (decrease of Cooper pair current). The positive magnetoresistance is dominating at low bias and low fields, as seen from Fig. 4(d). This is not unique for Bi-2201, but also occurs in big Bi-2212 junctions (see, e.g., Ref. 40) in which leakiness is the consequence of stacking faults (it is not present in small Bi-2212 mesas).²⁴ However, at larger bias the behavior becomes typical for single QP transport-

correlated suppression of both the peak and dip by a magnetic field [compare, e.g., with the data for Nb/AlAlOx/Nb junctions in Fig. 4(b) from Ref. 24].

V. DISCUSSION

Comparing our data of a very low- T_c cuprate with previous data of high- T_c cuprates^{16,27,32,34,35,41} reveals the following two universalities.

(i) All superconducting characteristics, including the temperature region of superconducting fluctuations are scaling down with T_c in the same proportion as for other cuprates.

(ii) The pseudogap characteristics remain similar in all types of cuprates, irrespective of T_c .

The reported disparity of the superconducting and pseudogap energy scales is difficult to reconcile with the precursor superconductivity scenario of the PG, for which one would expect $\Delta_{PG} \sim \Delta_{SG}$. Furthermore, due to the very low T_c in our case, the suppression of the critical temperature from $T^* \sim 170$ K to $T_c \lesssim 4$ K would require extraordinary large fluctuations. In the precursor scenario, the range of amplitude fluctuations should expand in the region $T \gtrsim T^* \sim 170$ K. However, from Fig. 4(c) it is seen that the superconducting amplitude fluctuations are decaying approximately exponentially $\propto \exp[-(T - T_c)/T_{fl}]$ at $T > T_c$ with a characteristic decay temperature $T_{fl} \sim 1$ K (compare also with similar data in Refs. 9 and 24 for other cuprates). Apparently fluctuations are bound to $T_c \lesssim 4$ K rather than to a much larger T^* . This is consistent with previous reports obtained by different techniques for different cuprates.^{3,6,9,10,23,24,27,42,43} The very low T_c in the studied cuprates provides a clear and unambiguous separation between superconducting fluctuation and pseudogap regions.

The temperature region of superconducting fluctuations is determined by the Ginzburg-Levanyuk parameter Gi . In the relevant two-dimensional case it is¹¹

$$\frac{T - T_c}{T_c} = Gi_{2D} \sim \frac{\Delta}{E_F}.$$

As reported, $\Delta_{\text{PG}} \sim 40$ meV and $T^* \sim 90\text{--}300$ K are similar to that in other cuprates.^{4,20,23,27,41} Furthermore, single-, double-, and triple-layer Bi-2201, Bi-2212, and Bi-2223 cuprates within the homologous family have similar normal state properties, Fermi energies E_F ,^{12–15} mobile hole densities, resistivities, anisotropy, etc.^{16–18,44} Therefore, Δ_{PG} cannot represent the universal superconducting pairing energy because in such a case Gi would be the same and superconductivity would be equally robust within the homologous family of cuprates. This is apparently not the case: The T_c and consequently the absolute value of fluctuation energy required for suppression of the superconducting phase coherence is largely different. The universal scaling of the fluctuation region with T_c suggests a similar relative strength of fluctuations for different cuprates, that is, the very low T_c in Bi-2201 is not due to extraordinary large phase fluctuations.

This conclusion brings up the important question of what causes the large variation of T_c within the homologous family of cuprates.^{12,45–49} Indeed, understanding what suppresses the T_c in Bi-2201 would provide a clue to understanding the high T_c in Bi-2212 and Bi-2223. Several suggestions were discussed in literature and perhaps one of the most common is that Bi-2201 is (more) disordered. For example, in Ref. 44 it was noted that pure low- T_c $\text{Bi}_2\text{Sr}_{2+x}\text{CuO}_{6+\delta}$ (note that it is different from $\text{Bi}_{2+x}\text{Sr}_{2-y}\text{CuO}_{6+\delta}$ studied here) had a slightly higher residual in-plane resistivity $\rho_{ab} \simeq 10^{-4}$ Ω cm than La-doped Bi-2201 with $T_c \sim 30$ K. The reduction of the electronic mean-free path below the coherence length may indeed increase the Gi parameter and thus enhance fluctuations.¹¹ For example, it is possible to quench superconductivity by intense ion or electron bombardment.⁹ On the other hand, superconductivity in cuprates occurs only in off-stoichiometric compounds as a result of doping (i.e., electronic defects). It is known that large variations of the residual resistivity in a given compound have practically no influence on T_c .¹⁷ Also Bi-2212 and Bi-2223 crystals with ρ_{ab} significantly larger than 10^{-4} Ω cm nevertheless show a high T_c .¹⁸ And the electronic surface inhomogeneity, studied by STM, is similar in Bi-2201 and Bi-2212 compounds.^{5,31} The crystal structure of $\text{Bi}_{2+x}\text{Sr}_{2-y}\text{CuO}_{6+\delta}$ crystals grown by the traveling solvent floating zone technique, as those studied here, were thoroughly investigated in Ref. 25 and it was demonstrated that the crystal order is very good. It is comparable to that in Bi-2212 and much better than in Bi-2223 and Hg-2223 crystals with the highest T_c . Thus, beyond doubt, a crystalline disorder is not the reason for low- T_c in Bi-2201.

Generally speaking, the T_c is determined by the density of states (DoS) at the Fermi level, which is related to the density of charge carriers (doping) and the details of the electronic structure, and by the coupling strength and the spectral function of the bosonic pairing glue. Factors that may affect the T_c are, in short: (i) An unequal doping in the inner and outer CuO_2 planes of multilayered cuprates, which is a well established factor affecting their T_c .⁴⁶

(ii) The stacking of CuO_2 layers in multilayered compounds may lead to a modification of the electronic band structure. For example, a (coherent) bonding-antibonding band splitting takes place in Bi-2212 in c -axis direction.⁵⁰ This affects the electronic DoS close to the Fermi energy. (iii) Similarly, the van Hove singularity in the flat regions of the Fermi surface near the edges of the Brillouin zone is affected^{12,48} and also (iv) the intralayer coupling is changed.⁴⁵ (v) An associated slight change in dimensionality may also affect the stability of the competing density wave order, coexisting with superconductivity.³¹ (vi) Furthermore, a modification of the structure leads to a modification of both the phononic spectrum⁴⁹ and the electron-boson coupling strength.⁴⁷ The connection between these electronic and bosonic factors with the critical temperature T_c is nonperturbative, that is, a small variation in these factors may lead to a significant variation of T_c . Therefore, it is likely that the large suppression of T_c in the high quality single crystals studied here is caused by the electronic and bosonic modifications within the homologous family of Bi-based cuprates, rather than by a disorder.

To summarize, combined intrinsic tunneling and transport measurements were performed on a single layer Bi-2201 cuprate with a very low $T_c \lesssim 4$ K. It was observed that the c -axis pseudogap characteristics ($\Delta_{\text{PG}} \simeq 40$ meV, $T^* \sim 90\text{--}170$ K, and $H^* \sim 200\text{--}300$ T) are the same as for Bi-2212 and Bi-2223 compounds with 20–30 times higher T_c , but all superconducting properties are scaling down with T_c : $\Delta_{\text{SG}} \simeq 0.55$ meV and $2\Delta_{\text{SG}}/k_B T_c \simeq 3.5 \pm 0.6$, the bosonic mode $\Omega_B \simeq 0.7$ meV and $\Omega_B/k_B T_c \simeq 2.2$, the upper critical field $H_{c2} \simeq 10$ T and $H_{c2}(T = 0 \text{ K})/T_c \simeq 2.5 \pm 1$ T/K, and the characteristic decay temperature for superconducting fluctuations (paraconductivity) $T_{\text{fl}} \simeq 1$ K and $T_{\text{fl}}/T_c \simeq 0.25$. The observed disparity is inconsistent with the precursor superconductivity scenario of the pseudogap. Therefore we conclude that the large $\Delta_{\text{PG}} \sim 40$ meV represents a different spin-singlet (e.g., antiferromagnetic,^{8,14} or a charge-and-spin density wave)³¹ order, which is universal for all cuprates and, most likely, competes with superconductivity. We also conclude that the low T_c in our Bi-2201 crystals is not caused by extraordinary strong thermal fluctuations at low T , nor by crystal defects, but is the consequence of a weaker coupling, leading to a small Cooper pair energy $2\Delta_{\text{SG}} \sim 1$ meV. However, what causes the large variation of the coupling strength within the homologous family of cuprates is still unclear. We emphasized that understanding the mechanism of T_c suppression in Bi-2201 is of significance for understanding the mechanism of high T_c in other cuprates.

ACKNOWLEDGMENTS

The work was supported by the Swedish Research Council and the EuroMagNET II (EC Contract No. 228043). One of us (A.M.) thanks Professor C. T. Lin for helpful discussions regarding the crystal growth.

*vladimir.krasnov@fysik.su.se

¹V. J. Emery and S. A. Kivelson, *Nature (London)* **374**, 434 (1995).

²Y. Wang, L. Li, and N. P. Ong, *Phys. Rev. B* **73**, 024510 (2006).

³J. L. Tallon and J. W. Loram, *Physica C* **349**, 53 (2001).

⁴V. M. Krasnov, *Phys. Rev. B* **65**, 140504(R) (2002).

- ⁵M. C. Boyer, W. D. Wise, K. Chatterjee, M. Yi, T. Kondo, T. Takeuchi, H. Ikuta, and E. W. Hudson, *Nat. Phys.* **3**, 802 (2007).
- ⁶S. Hüfner, M. A. Hossain, A. Damascelli, and G. A. Sawatzky, *Rep. Prog. Phys.* **71**, 062501 (2008).
- ⁷F. F. Balakirev, J. B. Betts, A. Migliori, I. Tsukada, Y. Ando, and G. S. Boebinger, *Phys. Rev. Lett.* **102**, 017004 (2009).
- ⁸S. Kawasaki, C. Lin, P. L. Kuhns, A. P. Reyes, and G. Q. Zheng, *Phys. Rev. Lett.* **105**, 137002 (2010).
- ⁹H. Alloul, F. Rullier-Albenque, B. Vignolle, D. Colson, and A. Forget, *Europhys. Lett.* **91**, 37005 (2010); F. Rullier-Albenque, H. Alloul, and G. Rikken, *Phys. Rev. B* **84**, 014522 (2011).
- ¹⁰J. Chang *et al.*, *Nat. Phys.* **8**, 751 (2012).
- ¹¹A. I. Larkin and A. A. Varlamov, *Theory of Fluctuations in Superconductors* (Oxford University Press, New York, 2009).
- ¹²A. D. Palczewski *et al.*, *Phys. Rev. B* **78**, 054523 (2008).
- ¹³T. Kondo, Y. Hamaya, A. D. Palczewski, T. Takeuchi, J. S. Wen, Z. J. Xu, G. Gu, J. Schmalian, and A. Kaminski, *Nat. Phys.* **7**, 21 (2011).
- ¹⁴R. H. He *et al.*, *Science* **331**, 1579 (2011).
- ¹⁵Y. Okada, T. Kawaguchi, M. Ohkawa, K. Ishizaka, T. Takeuchi, S. Shin, and H. Ikuta, *Phys. Rev. B* **83**, 104502 (2011).
- ¹⁶S. I. Vedenev, A. G. M. Jansen, E. Haanappel, and P. Wyder, *Phys. Rev. B* **60**, 12467 (1999).
- ¹⁷Y. Ando, G. S. Boebinger, A. Passner, N. L. Wang, C. Geibel, and F. Steglich, *Phys. Rev. Lett.* **77**, 2065 (1996).
- ¹⁸T. Watanabe, T. Fujii, and A. Matsuda, *Phys. Rev. Lett.* **79**, 2113 (1997).
- ¹⁹R. Kleiner and P. Müller, *Phys. Rev. B* **49**, 1327 (1994).
- ²⁰Y. Yamada, K. Anagawa, T. Shibauchi, T. Fujii, T. Watanabe, A. Matsuda, and M. Suzuki, *Phys. Rev. B* **68**, 054533 (2003).
- ²¹A. Yurgens, D. Winkler, T. Claeson, S. Ono, and Y. Ando, *Phys. Rev. Lett.* **90**, 147005 (2003).
- ²²H. Kashiwaya, T. Matsumoto, H. Shibata, H. Eisaki, Y. Yoshida, H. Kambara, S. Kawabata, and S. Kashiwaya, *Appl. Phys. Express* **3**, 043101 (2010).
- ²³V. M. Krasnov, *Phys. Rev. B* **79**, 214510 (2009).
- ²⁴V. M. Krasnov, H. Motzkau, T. Golod, A. Rydh, S. O. Katterwe, and A. B. Kulakov, *Phys. Rev. B* **84**, 054516 (2011).
- ²⁵B. Liang, A. Maljuk, and C. T. Lin, *Physica C* **361**, 156 (2001).
- ²⁶V. M. Krasnov, M. Sandberg, and I. Zogaj, *Phys. Rev. Lett.* **94**, 077003 (2005).
- ²⁷A. N. Lavrov, Y. Ando, and S. Ono, *Europhys. Lett.* **57**, 267 (2002).
- ²⁸P. A. Warburton *et al.*, *J. Appl. Phys.* **95**, 4941 (2004); M. H. Bae, M. Sahu, H. J. Lee, and A. Bezryadin, *Phys. Rev. B* **79**, 104509 (2009).
- ²⁹N. Miyakawa, J. F. Zasadzinski, S. Oonuki, M. Asano, D. Henmi, T. Kaneko, L. Ozyuzer, and K. E. Gray, *Physica C* **364-365**, 475 (2001).
- ³⁰G. L. de Castro, Ch. Berthod, A. Piriou, E. Giannini, and Ø. Fischer, *Phys. Rev. Lett.* **101**, 267004 (2008).
- ³¹W. D. Wise, M. C. Boyer, K. Chatterjee, T. Kondo, T. Takeuchi, H. Ikuta, Y. Wang, and E. W. Hudson, *Nat. Phys.* **4**, 696 (2008).
- ³²T. Kato, H. Funahashi, H. Nakamura, M. Fujimoto, T. Machida, H. Sakata, S. Nakao, and T. Hasegawa, *J. Supercond. Nov. Magn.* **23**, 771 (2010).
- ³³M. Kugler, Ø. Fischer, Ch. Renner, S. Ono, and Y. Ando, *Phys. Rev. Lett.* **86**, 4911 (2001).
- ³⁴G. Yu, Y. Li, E. M. Motoyama, and M. Greven, *Nat. Phys.* **5**, 873 (2009).
- ³⁵S. Ideta *et al.*, *Phys. Rev. B* **85**, 104515 (2012).
- ³⁶Z. Hao and A. V. Chubukov, *Phys. Rev. B* **79**, 224513 (2009).
- ³⁷S. O. Katterwe, A. Rydh, and V. M. Krasnov, *Phys. Rev. Lett.* **101**, 087003 (2008).
- ³⁸J. P. Carbotte, *Rev. Mod. Phys.* **62**, 1027 (1990).
- ³⁹T. Kawakami, T. Shibauchi, Y. Terao, M. Suzuki, and L. Krusin-Elbaum, *Phys. Rev. Lett.* **95**, 017001 (2005).
- ⁴⁰N. Morozov, L. Krusin-Elbaum, T. Shibauchi, L. N. Bulaevskii, M. P. Maley, Yu. I. Latyshev, and T. Yamashita, *Phys. Rev. Lett.* **84**, 1784 (2000).
- ⁴¹A. Dubroka *et al.*, *Phys. Rev. Lett.* **106**, 047006 (2011).
- ⁴²L. S. Bilbro, R. Valdes Aguilar, G. Logvenov, O. Pelleg, I. Božović, and N. P. Armitage, *Nat. Phys.* **7**, 298 (2011).
- ⁴³M. S. Grbic, M. Požek, D. Paar, V. Hinkov, M. Raichle, D. Haug, B. Keimer, N. Barišić, and A. Dulčić, *Phys. Rev. B* **83**, 144508 (2011).
- ⁴⁴S. Ono and Y. Ando, *Phys. Rev. B* **67**, 104512 (2003).
- ⁴⁵S. Chakravarty, H. Y. Kee, and K. Völker, *Nature (London)* **428**, 53 (2004).
- ⁴⁶H. Kotegawa, Y. Tokunaga, K. Ishida, G.-q. Zheng, Y. Kitaoka, H. Kito, A. Iyo, K. Tokiwa, T. Watanabe, and H. Ihara, *Phys. Rev. B* **64**, 064515 (2001).
- ⁴⁷H. Matsui, T. Sato, T. Takahashi, H. Ding, H.-B. Yang, S.-C. Wang, T. Fujii, T. Watanabe, A. Matsuda, T. Terashima, and K. Kadowaki, *Phys. Rev. B* **67**, 060501(R) (2003).
- ⁴⁸S. Koikegami and T. Yanagisawa, *J. Phys. Soc. Jpn.* **75**, 034715 (2006).
- ⁴⁹S. Johnston, F. Vernay, B. Moritz, Z.-X. Shen, N. Nagaosa, J. Zaanen, and T. P. Devereaux, *Phys. Rev. B* **82**, 064513 (2010).
- ⁵⁰A. A. Kordyuk, S. V. Borisenko, T. K. Kim, K. A. Nenkov, M. Knupfer, J. Fink, M. S. Golden, H. Berger, and R. Follath, *Phys. Rev. Lett.* **89**, 077003 (2002).